Biochemical and Biophysical Research Communications 440 (2013) 215–221

Contents lists available at ScienceDirect

Biochemical and Biophysical Research Communications

journal homepage: www.elsevier.com/locate/ybbrc

# Surface-induced conformational and functional changes of bone morphogenetic protein-2 adsorbed onto single-walled carbon nanotubes

Ziyu Li [a,b], Qi Gan [b], Wenjing Zhang [b], Jing Zhang [b], Yuan Yuan [a,b,*], Changsheng Liu [a,b,*]

[a] The State Key Laboratory of Bioreactor Engineering, East China University of Science and Technology, Shanghai 200237, PR China
[b] Key Laboratory for Ultrafine Materials of Ministry of Education and Engineering Research Center for Biomedical Materials of Ministry of Education, East China University of Science and Technology, Shanghai 200237, PR China

ARTICLE INFO

*Article history:*
Received 30 August 2013
Available online 18 September 2013

*Keywords:*
BMP-2
Conformation
Functionality
Single-walled carbon nanotubes

ABSTRACT

Efficient immobilization of bone morphogenetic protein-2 (BMP-2) onto matrix is of crucial importance in the development of BMP-2-based bone tissue scaffold/implant. This often ties with precise control of desirable protein conformation and retention of protein activity. Recently, great attentions were paid to the regulation of protein conformation by tailoring the nanoscale surface properties. In this contribution, with hydrophilic COOH- and hydrophobic $CH_3$-terminated single-walled carbon nanotubes (SWNTs-COOH and SWNTs-$CH_3$) as models, we investigated the nanoscale interface-induced changes of adsorption dynamics, conformation, and bioactivity of recombinant human BMP-2 (rhBMP-2). Our data showed that SWNTs-COOH and SWNTs-$CH_3$ bound rapidly to and induced unfolding of rhBMP-2 molecules, which promoted their interactions with corresponding receptors on cell surface and thus enhanced their bioactivities. In contrast, rhBMP-2 showed stronger affinity to the COOH-terminated surface than that terminated with $CH_3$ groups, while better enhanced bioactivity on the SWNTs-$CH_3$ surfaces. After released from SWNTs, the unfolded rhBMP-2 refolded and their activities from SWNTs-COOH and SWNTs-$CH_3$ were reduced to 90% and 70% of the native rhBMP-2, respectively. Based on these results obtained, a model of the binding characteristics of rhBMP-2 onto SWNTs with different chemistry is presented. This study demonstrates the possibility of simple tailor-made nanoscale chemical surfaces to modulate the binding, conformation and bioactivity of BMP-2, allowing fabrication of BMP-2-based bone tissue scaffolds with high osteoinductivity and low BMP-2 dosage.



## 1. Introduction

As one of the transforming growth factor (TGF-β) superfamily, bone morphogenetic protein-2 (BMP-2) has been considered as the most notable cytokines to enhance bone formation and bone tissue reconstruction. Since 2002, recombinant human BMP-2 (rhBMP-2) has been approved by US Food and Drug Administration to use in clinics for fracture healing, spinal fusion, and implant fixation [1,2]. Unfortunately, due to their poor solubility, short biological half-life, and rapid local clearance under physiological conditions *in vivo*, rhBMP-2 often exhibits poor localized therapeutic efficacy so that large dosage are generally unavoidable [3,4]. To address these problems, rhBMP-2 were currently encapsulated in some localized and sustained releasing matrix, mimicking their surface-associated behaviors in native physiology [5,6]. However, efficient immobilization of rhBMP-2 onto carriers with low dosage and desirable *in vivo* regenerating action stays as a major challenge in bone regeneration research and practice [6,7]. The required BMP-2 level in humans, even the FDA-approved collagen sponge-incorporated ones, is much higher (over six orders of magnitude higher) than what is used in *in vitro* cell level evaluation and *in vivo* animal studies [2,6].

The surface-induced regulation of the conformation and function of proteins have recently attracted great attentions [8–11]. These changes are strongly dependent on both the nature of the adsorbed proteins and the physicochemical characteristics of the solid surfaces, including chemistry [8], size [9] and curvature [10]. Such surface-mediated protein changes become increasingly important at the nanoscale for their comparable size to proteins. For example, Karajanagi et al., found that upon adsorption on single-walled carbon nanotubes, both α-chymotrypsin and soybean peroxidase underwent obvious structure change, resulting in nearly 99% and 50% deactivation, respectively [11]. With silica nanoparticles of various diameters and curvatures as models, BSA was found to become less ordered on large nanoparticles, while Fg subgroups were denatured to a greater extent on small nanoparticles [8]. Poly(acrylic acid)-conjugated Au nanoparticles could

* Corresponding authors. Address: East China University of Science and Technology, Box 112, No. 130, Meilong Road, Shanghai 200237, PR China. Fax: +86 21 64251358.
*E-mail addresses:* yyuan@ecust.edu.cn (Y. Yuan), liucs@ecust.edu.cn (C. Liu).

0006-291X/$ - see front matter © 2013 Elsevier Inc. All rights reserved.
http://dx.doi.org/10.1016/j.bbrc.2013.09.036

induce the unfolding of fibrinogen and thus promoted Mac-1 receptor activation and inflammation [9]. Given the role played by the nano-scaled surface in the regulation of the microstructure and bioactivity of the proteins, it is desirable to modulate the surface properties of the substrate to realize desirable immobilization of rhBMP-2. However, till now, relatively little is known about the structure, function, and spatial orientation of rhBMP-2 on the adsorbed matrixes and how such surface changes tailor the conformation and bioactivity of rhBMP-2.

We herein studied the nanotube surface-induced changes on the conformational structure and bioactivity of rhBMP-2. Single-walled carbon nanotubes (SWNTs) with unique geometry and tunable hydrophilicity were selected as the model substrate because it is a widely used model to investigate such protein-nanoscaled surface interaction [11,12]. The adsorption dynamics, the secondary structure, and thereby the bioactivities of rhBMP-2 on both hydrophobic $CH_3$-terminated and the hydrophilic COOH-terminated SWNTs (SWNTs-$CH_3$, SWNTs-COOH) were investigated in details. Based on our best knowledge, this is the first study that examines how rhBMP-2 interacts with nanoscale surfaces with defined chemistry and topography. For comparison, the adsorption behaviors of BSA were also studied in this study.

## 2. Experimental

### 2.1. Materials

Recombinant human bone morphogenetic protein (rhBMP-2, purity >95%, IEP = 8.1) was generously provided by Shanghai Rebone Biomaterial Co. Ltd. (Shanghai, China). BCA kit and 2-(4-amidinophenyl)-6-indolecarbamidine dihydrochloride (DAPI) were purchased from Beyotime Biotech. (Jiangsu, China). High purity SWNTs-$CH_3$ were obtained from Timesnano (purity >95%). C2C12, a myoblastic precursor cell with osteoblastic potential, was purchased from American Type Culture Collection (ATCC). Anti-BMP-2 antibody (R&D Systems Inc., Minneapolis, USA) and FITC-conjugated goat-anti-mouse IgG were obtained from Sigma–aldrich (CA, USA). All chemicals were of analytical grade.

### 2.2. Characterization

The zeta-potentials of the native protein, SWNTs-COOH and SWNTs-$CH_3$ were measured by a Zetasizer Nano ZS instrument in neutral environment at 25 °C. TEM and high-resolution TEM (HRTEM) were performed on a transmission electron microscope (JEM-2100, Japan) with a field emission gun operating at 200 kV.

### 2.3. Adsorption behavious of protein onto SWNTs

To improve the dispersion, SWNTs were pretreated by an organic phase/aqueous phase replacement approach according to the previous reports [11]. SWNTs were dispersed in PBS with the concentration of 1 mg/mL by sonicating for 10 min. The SWNTs aliquot was then exposed to the protein solution (0.1–1.0 mg/L) freshly prepared in PBS. The mixture was moved to a shaker (at 100 rpm) for further incubation at 25 °C to prevent autolysis. After incubation, the complex of substrate and protein were centrifuged at 10,000 rpm using a micro-centrifuge and the supernatant was removed. The amount of protein loaded onto the substrate was determined by measuring the difference of the concentrations of protein in the solution or supernatant before and after SWNTs exposure.

### 2.4. Conformational assessment of rhBMP-2

Infrared analysis of surface-bound protein was conducted using a Golden Gate ATR accessory in a Nicolet 6700 spectrometer. The rhBMP-2 adsorbed onto SWNTs were lyophilized and the lyophilized protein-substrate composite (1 mg) was ground to IR grade KBr of powder (~40–50 mg). About 30 mg of pellet was transferred into the FT-IR chamber. The FT-IR spectrum of the unfunctionalized SWNTs-$CH_3$ and SWNTs-COOH were obtained in an identical manner. The spectrum of the bare substrate was subtracted from that of the corresponding protein-bound substrate to obtain the spectrum of the adsorbed protein.

### 2.5. Evaluation of the bioactivity of the rhBMP-2

C2C12 cells were cultured in 37.5 $cm^2$ flasks with Dulbecco's modified Eagle's medium (DMEM, we called growth medium) containing 10% fetal calf serum, antibiotics (100 U/mL penicillin-G, and 100 mg/mL streptomycin)) at humidified atmosphere of 5% $CO_2$/95% air until confluence, then detached with 0.25% trypsin/0.03% ethylenediamine tetraacetic acid (EDTA), and the cell density was calculated and used at the desired density in later experiments.

Batch experiments were conducted to measure the ALP activity of the free rhBMP-2, rhBMP-2 adsorbed onto the substrate (SWNTs-COOH and SWNTs-$CH_3$), and the rhBMP-2 released from the complex (rhBMP-2/SWNTs-$CH_3$ and rhBMP-2/SWNTs-COOH), respectively. The concentration of rhBMP-2 of all the experiment was kept at 2.5 μg/mL. A blank experiment with buffer only was carried out. Each group was performed in quintuplicate.

ALP activity was measured using p-nitrophenyl phosphate (Sangon, Shanghai, China) as the substrate as previously described. Briefly, C2C12 cells were seeded at a density of $1.2 \times 10^4$ per well into 96-well plates. After 24 h incubation in growth medium, cells were washed with PBS twice and refreshed with 200 μL maintenance medium (DMEM containing 2% fetal calf serum) in the presence of rhBMP-2 with or without SWNTs. After a 2 h incubation, the maintenance medium including rhBMP-2/SWNTs was removed, refreshed with 200 μL maintenance medium, and put back to the incubator. At the end of 72 h incubation, 50 μL 1% Nonidet P-40 (NP-40) solution was added to each well and wait for 1 h to obtain cell lysate. Further, 0.1 mL of 1 mg/mL p-nitrophenyl phosphate substrate solution (pH = 9.0) composed of 0.1 M glycine, 1 mM $MgCl_2 \cdot 6H_2O$ was added and incubated for another 15 min at 37 °C. The reaction was then quenched by adding 0.1 mL of 0.1 M NaOH. The absorbance of ALP was quantified at the wavelength of 405 nm using a microplate reader (SPECTRAmax 384, Molecular Devices, USA). ALP activity was expressed as 405 nm OD value per min per total protein.

### 2.6. Binding to its receptor of cell surface of rhBMP-2 on SWNTs

Cells were pre-cultured on chamber slides with 0.01% poly-L-lysine (PLL) for 24 h. After that, medium was supplemented with free rhBMP2 and hydrophobic/hydrophilic SWNTs. After another 4 h incubation, cells were then placed on ice for 5 min, washed twice with ice cold PBS. Cells were fixed with 1% glutaraldehyde for 15 min at 4 °C. The BSA blocking buffer solution (3%) was then added and samples were further incubated at 37 °C for 1 h. After washing with PBS twice, cells were incubated with anti-BMP2 antibody (R&D Systems Inc., Minneapolis, USA) for 1 h at 37 °C and the cultures were placed at 4 °C for 1 h. For rhBMP-2 staining, cells were incubated with a dilution of FITC-conjugated goat-anti-mouse IgG for 1 h at RT. DAPI solution was added to stain cell nucleus for 5 min. After washing with PBS for 5 times with 3 min interval, slides were covered with 50% glycerol in water.

RhBMP-2 and cell nucleus were monitored with confocal laser scanning microscope (Nikon A1R) inspired by blue and green light, respectively.

### 2.7. Statistical analysis

All numerical data were expressed as the mean ± standard deviation, with similar results obtained in each experiment. Statistical analysis was performed with one-way analysis of variance (ANOVA). A value of $p < 0.05$ was considered statistically significant.

## 3. Results

### 3.1. Physicochemical properties of the SWNTs

TEM images (Fig. 1) revealed well-dispersed SWNTs-$CH_3$ and SWNTs-COOH in aqueous solution. The single bundle of SWNTs were about 6–8 nm, comparable to the size of proteins. The zeta potentials of the SWNTs-$CH_3$ and SWNTs-COOH exhibited positive and negative in nature (Table. S1). FTIR analysis (Fig. S1) confirmed the existence of –COOH on SWNTs after –COOH functionalization by showing a peak at 1650 $cm^{-1}$, corresponding to the acid carbonyl stretching vibration [13]. A great reduction of contact angle was also found (Table.S1) after this surface modification. But, the specific surface area of the SWNTs had only slight alteration after modification.

### 3.2. Protein under investigation

With a molecular weight of 26 kDa and three-dimension of 7 nm × 3.5 nm × 3 nm, BMP-2 is a homodimer linked with interchain disulfide bridges in its biologically active form (Fig. S2). The rigid cystine-knots consisting of three intrachain disulfide bridges are formed between six cysteine residues and the interchain disulfide bridges enable BMP-2 to show striking stability [14,15].

It is well-established that BMP-2 signals through specific cellular receptors composed of two types of serine-kinase receptor chains [16]. The 'wrist' epitope assembled around the central α-helix binds the type I A (BMPR-I A) and typeI B (BMPR-I B) receptors by activating the cellular SMAD 1/5 signaling pathway. While the 'knuckle' epitope located at the back of the hand near the outer finger segment binds to BMP-2 receptor type BMPR-II or ActR-II by activating type. It is also believed that BMP-2 often activates its cellular receptor via a high-affinity 'wrist' epitope-BMPR-IA interaction and a low-affinity 'knuckle' epitope-BMPR-II interaction, especially the former. As indicated in Fig. S2, one monomer mainly provides residues Val 26, Asp 30, Trp 31 from the long loop connecting strands β2 and β3, and the other contributes residues Ile 62, Leu 66, Asn 68 and Ser 69 in helix α3 [15]. Therefore, to attain immobilized BMP-2 with high activity, it is necessary to ensure the accessibility of these determinants for ligand–receptor interactions.

### 3.3. Adsorption behavious of rhBMP-2 on SWNTs

Fig. 2 shows the isothermal adsorption profiles of rhBMP-2 onto SWNTs-$CH_3$ and SWNTs-COOH. From Fig. 2(A), it can be seen that rhBMP-2 exhibited a very rapid adsorption toward both SWNTs-$CH_3$ and SWNTs-COOH, with almost 90% adsorption observed within the initial 10 min.

Although the adsorption of rhBMP-2 on SWNTs$CH_3$ and SWNTs-COOH followed similar pseudo-saturation behavior as shown in Fig. 2(B) and Fig. 2(C), the maximum loading of rhBMP-2 on the two substrates were quite different. A near 3-fold increase of maximum loading was observed on the SWNTs-COOH surface (2.67 mg rhBMP-2/ $m^2$ SWNTs-COOH) than that on the SWNTs-$CH_3$ surface (0.64 mg rhBMP-2/ $m^2$ SWNTs-COOH). This suggests that various protein-surface interactions exist due to their different chemistry of substrates. In contrast, BSA showed a slight higher adsorption amount onto SWNTs-$CH_3$ (0.99 mg BSA/$m^2$ SWNTs-$CH_3$) than that onto SWNTs-COOH (0.78 mg BSA/$m^2$ SWNTs-COOH) (Fig. S3(c)). We believed that such different adsorption behavior was mainly

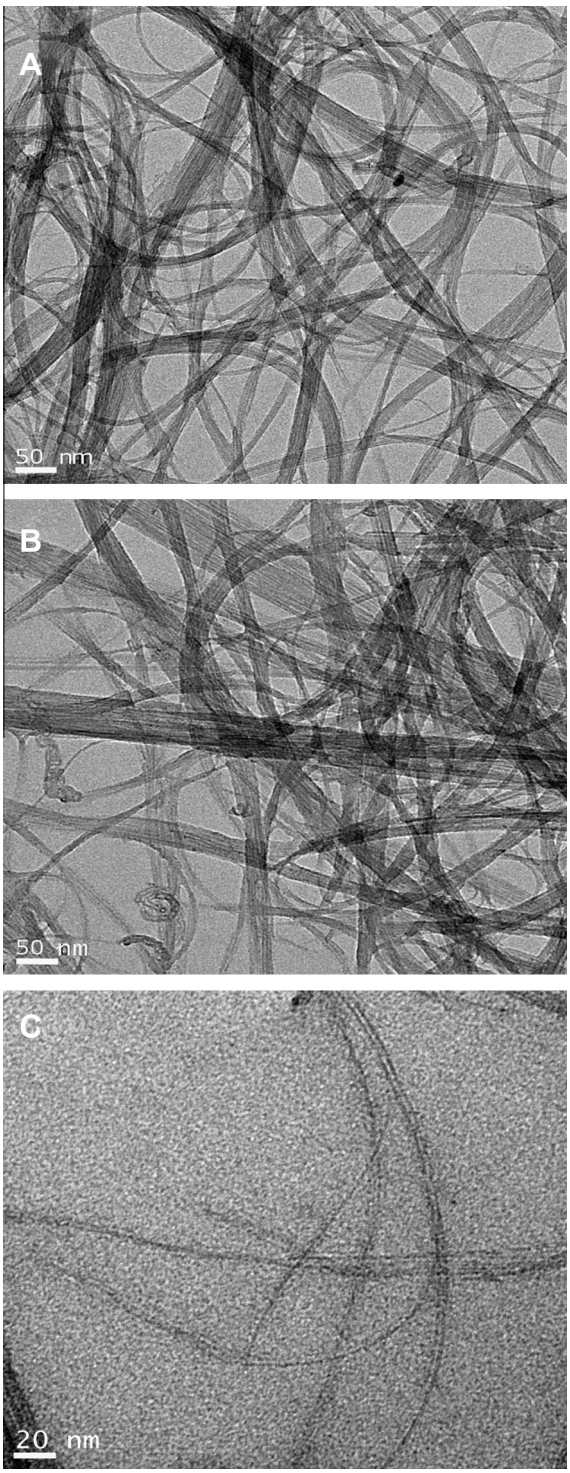


**Fig. 1.** TEM images of (A) hydrophobic SWNTs-$CH_3$, (B) hydrophilic SWNTs-COOH, and (C) a magnified view of (B).

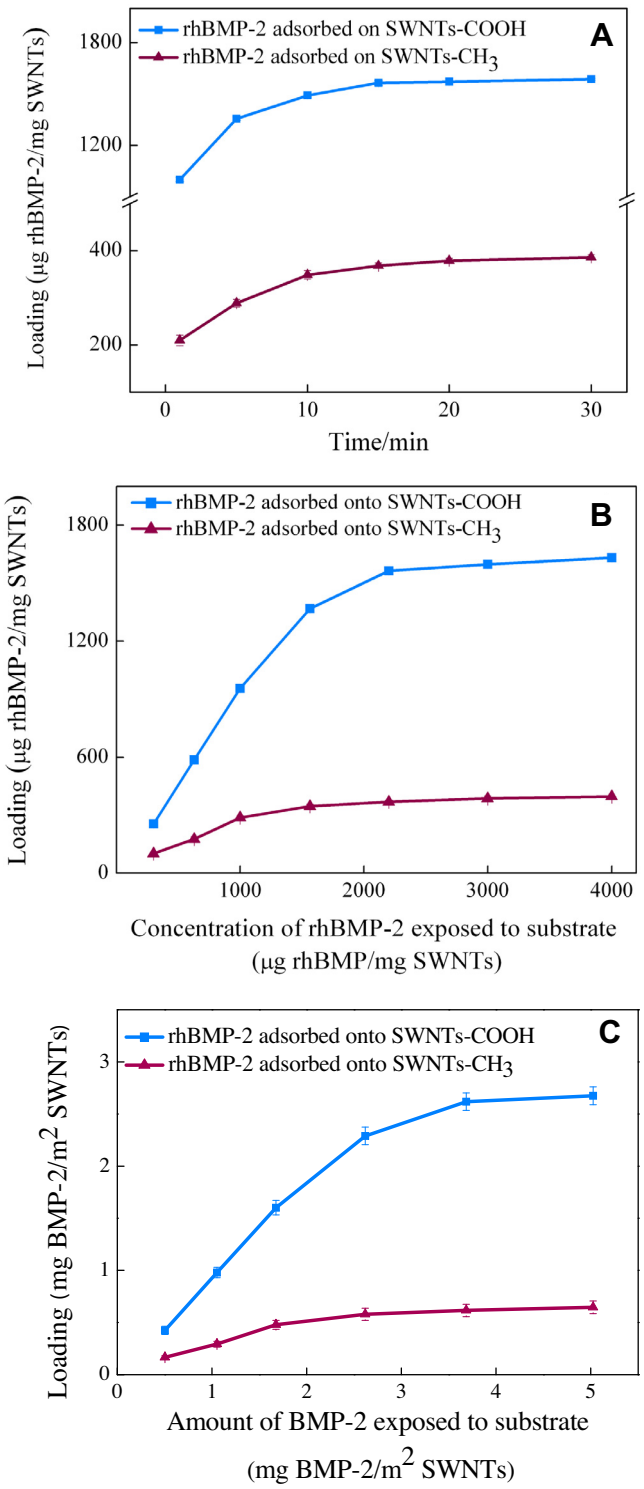


**Fig. 2.** (A) Protein adsorption dynamics for rhBMP-2 adsorbing onto SWNTs (The concentrations of rhBMP-2 were kept at 0.5 mg/mL. The loading-concentration curve of rhBMP-2 on SWNTs surfaces on mass basis (B) and on surface area basis (C). (The time for adsorption was kept at 30 min. The experiment was repeated three times and the standard deviation was calculated ($n = 3$).

related to the inherent characteristics of BSA and rhBMP-2. As listed in Table S1, at pH 7.4, rhBMP-2 is positive charged while BSA is negative charged. In order to avoid undesirable protein–protein interactions on the SWNTs surface, half of the maximum loading amount of each protein adsorption onto the specific substrate was taken in the following section.

### 3.4. Conformational assessment

The amide I band centered at 1700–1600 $cm^{-1}$, largely due to C=O stretching vibrations, was used for quantitative estimation the secondary structural feature of protein. The secondary structural features were calculated from the amide I spectra using the second-derivative method (see Suppoting information Fig. S4 for the assignments of peaks to secondary structural elements) as previous reports [17]. The differences in secondary structure between the free protein and the adsorbed proteins are presented by the magnitudes of changes in α-helix and β-sheet content.

It can be seen from Table 1, upon adsorption, rhBMP-2 underwent significant unfolding on both SWNTs. However, the variations of the secondary structure were totally different. Specifically, after adsorbed on SWNTs-$CH_3$ surface, rhBMP-2 greatly lost the β-sheet/β-turn characters (with only 11.8% remaining), but the α-helical structure (19.3%) kept nearly intact. However, when adsorbed onto the SWNTs-COOH surface, rhBMP-2 suffered reduction of both α-helical (8%) and β-sheet content (13%) simultaneously. In contrast, the sum of changes in α-helix and β-sheet/β-turn contents of rhBMP-2 adsorbed onto the SWNTs-$CH_3$ and SWNT-COOHs were 33.2% and 21%, respectively. This obvious disparity of unfolding effect induced by varied SWNTs could attribute to the different interactions between rhBMP-2 and the contacted substrates, which is discussed in the following section.

### 3.5. Bioactivity changes of the rhBMP-2 adsorbed onto SWNTs

As an osteoinductive growth factor, the binding to its receptors on cell surface is the first and essential step for the osteoinductive process of rhBMP-2. So, here we investigated the binding of the adsorbed-rhBMP-2 with its cellular receptor according to the previous report [18]. The rhBMP-2 localized on the cell surface was directly detected by the immunofluorescent staining via anti-rhBMP-2 primary antibody and FITC-conjugated goat-anti-mouse IgG. The cell nucleus was stained with DAPI served for cell localization. As shown in Fig. 3(A) and (B), compared with the free rhBMP-2 (Fig. S5), the fluorescence intensities of adsorbed rhBMP-2 were greatly enhanced by both types of surfaces.

ALP, a typical osteoblast-specific marker, has been implicated as a key factor in osteoblast differentiation and was widely used to quantitatively investigate the bioactivity of rhBMP-2 [19]. Therefore, we next tested the ALP expression levels of the rhBMP-2 before and after adsorbed at the same concentration. As shown in Fig. 3(C), compared with the free rhBMP-2, ALP activity of rhBMP-2/SWNTs-$CH_3$ and rhBMP-2/SWNT-COOHs were increased around 51% and 23%, respectively, exhibiting the similar trend with the interactions of rhBMP-2-receptors on the surface.

We further explored and compared the bioactivity of rhBMP-2 after released from different substrates. It was found that, there was striking distinction of the ALP expression of the rhBMP-2 released from the two different types of surface, as shown in Fig. 3(D). The ALP expression of rhBMP-2 released from the SWNTs-COOH surface was comparable to that of the native-like rhBMP-2, while decreased by about 30% for those released from SWNTs-$CH_3$. Further compared the ALP expression of the rhBMP-2 onto the SWNTs-$CH_3$ and SWNTs-COOH (Fig. 3(C)) at the same concentration, it can be concluded that the bioactivity of rhBMP-2 exhibited nearly 2-fold reduction after released from the SWNTs-$CH_3$ matrix while preserved 75% of its activity for SWNTs-COOH. These findings suggested that the rhBMP-2 molecules, particularly those released from the SWNTs-$CH_3$ surface, were somewhat denatured after release, due to the refolding of the rhBMP-2 in aqueous environment. This was confirmed by the FTIR spectra and Far-UV circular dichroism data of rhBMP-2 released from the substrate (Table 1 and Fig. S6).

**Table 1**
Secondary structure of rhBMP-2 (free, adsorbed onto and released from SWNTs) as determined by FT-IR Spectroscopy.

| Sample/Structure (%) | β-Sheet/β-turn | α-Helical | Change of the folding structure |
|---|---|---|---|
| Free rhBMP-2 | 44.0 | 18.3 | 0 |
| rhBMP-2 adsorbed onto SWNTs-$CH_3$ | 11.8 | 19.3 | 33.2 |
| rhBMP-2 adsorbed onto SWNTs-COOH | 36.0 | 5.3 | 21.0 |
| rhBMP-2 released from SWNTs-$CH_3$ | 48.2 | 28.6 | 14.5 |
| rhBMP-2 released from SWNTs-COOH | 42.1 | 16.8 | 3.4 |

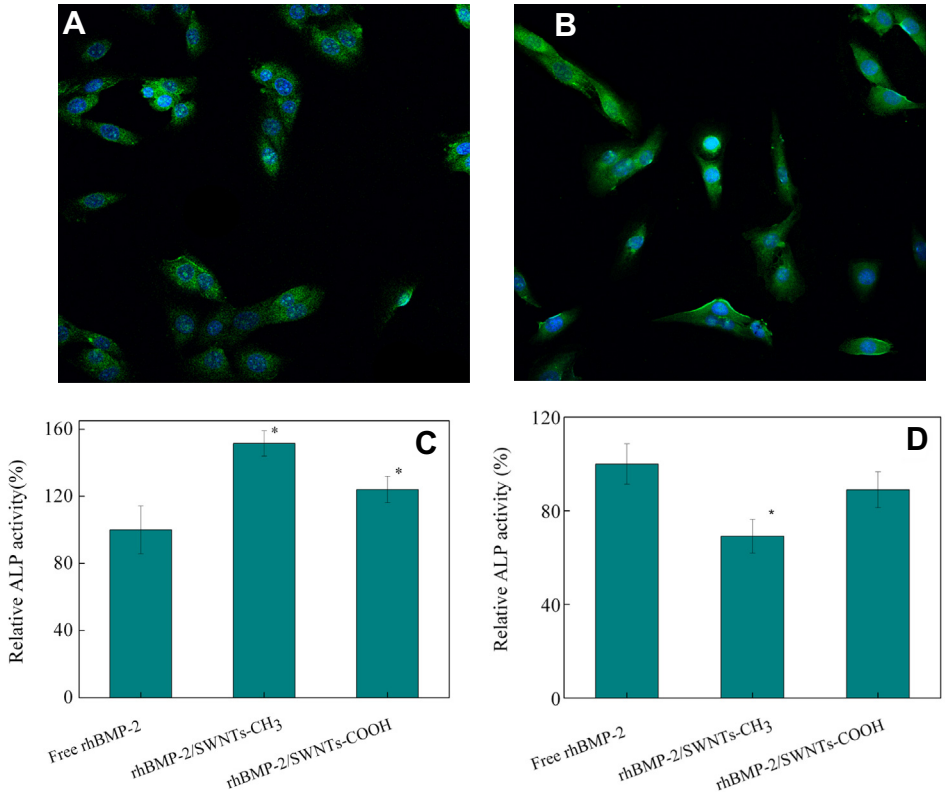


**Fig. 3.** Binding capacity of rhBMP-2 adsorbed onto SWNTs to its cellular receptor on cell surface. (A) rhBMP-2/SWNTs-$CH_3$, (B) rhBMP-2/SWNTs-COOH. C2C12 cell were pretreated with rhBMP-2/SWNTs-COOH or rhBMP-2/SWNTs-$CH_3$ at 2.5 μg/mL rhBMP-2 in the culture medium for 2 h. RhBMP-2 was detected with anti-rhBMP-2 antibody and FITC labeled anti-mouse IgG (green) and cell nuclei were stained with DAPI (blue) for cell orientation (400×). ALP activity of the complex of rhBMP-2/SWNTs (C) and the rhBMP-2 after releasing from the complex of rhBMP-2/SWNTs (D). Cells were cultured for 2 h with the complex of rhBMP-2/SWNTs-$CH_3$, rhBMP-2/SWNTs-COOH, and the rhBMP-2 released from the complex of rhBMP-2/SWNTs-$CH_3$ and rhBMP-2/SWNTs-COOH, respectively. ALP was measured after 72 h using soluble p-nitrophenylphosphate. The value represents the mean ± standard deviation ($n$ = 5). (For interpretation of the references to color in this figure legend, the reader is referred to the web version of this article.)

## 4. Discussion

In this study, the adsorption behavior, conformation and bioactivity of rhBMP-2 adsorbed onto hydrophilic SWNTs-COOH and hydrophobic SWNTs-$CH_3$ were investigated. The results here indicated that rhBMP-2 showed a much higher binding saturation value onto the hydrophilic compared to the hydrophobic surface. Moreover, an obviously adsorption-induced unfolding of rhBMP-2 on both the SWNTs-COOH and SWNTs-$CH_3$ surfaces were observed. And the deformations on the SWNTs-COOH and SWNTs-$CH_3$ surfaces all facilitated the interactions between rhBMP-2 and its receptors on cell surface and enhanced the corresponding ALP expression, in particular for the SWNTs-$CH_3$ surface. But after released from the SWNTs-COOH and SWNTs-$CH_3$ surfaces, the SWNTs-induced unfolding of rhBMP-2 disappeared and the bioactivity of rhBMP-2 reduced to 90% and 70% of that of the native rhBMP-2, respectively.

This noticeable surface chemistry-dependent conformation and bioactivity of rhBMP-2 on SWNTs aroused our attentions. It is well-recognized that the primary interactions between the protein residue and the substrate surface are dependent on the electrostatic potential, hydrophobic interaction and surface area of contact [20]. A high opposite electrostatic potential will strengthen the protein-substrate interactions, so will the high hydrophobic interactions and the large contact surface area. Just like other proteins, BMP-2 is comprised of many different amino acids with various polarities and charges. Therefore, the protein chains may exhibit varied affinity to hydrophobic and hydrophilic surfaces. BMP-2 is hydrophobic in nature and its hydrophobic packing is the most abundant form of subunit interactions in the BMP-2 dimer [21]. The high-affinity binding of the 'wrist' epitope of BMP-2 and the BRI A receptor plays an important role during the cellular response and almost 60% of the contact surface area is provided by its hydrophobic residues [22]. Therefore, consistent with the previous report [9], the adsorption-induced unfolding might lead to the alteration of ligand-receptor binding and thus the osteoactivity of BMP-2.

Based on the previous investigations and the results presented here, a simple model was proposed, as illustrated in Fig. 4. In

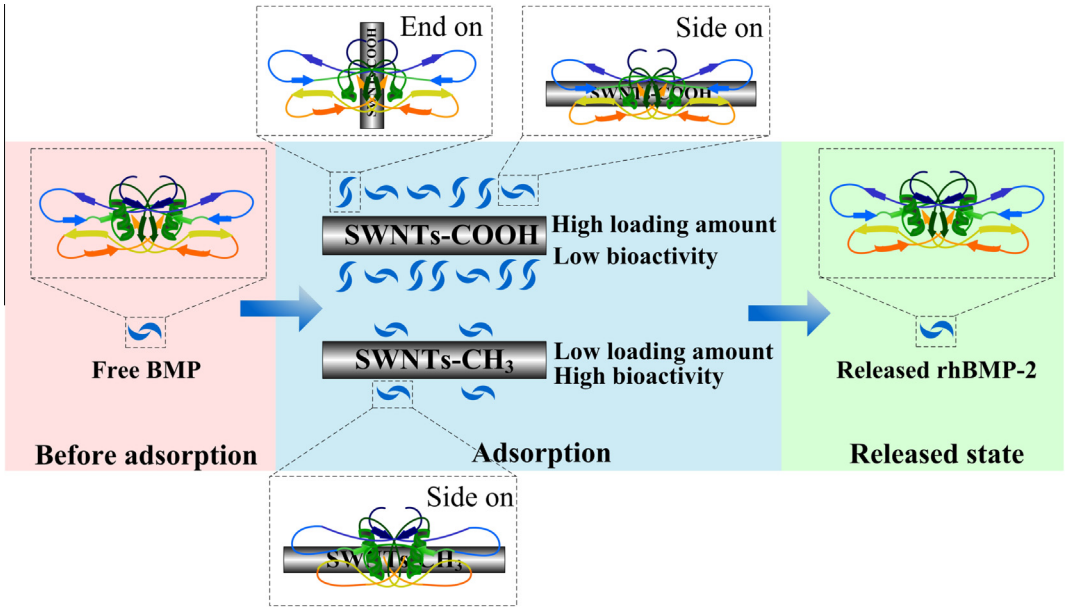


**Fig. 4.** Schematic diagram of the interactions of rhBMP-2 and SWNTs with different surface chemistry.

aqueous solution, in order to create strong interaction with water molecules, rhBMP-2 molecule exhibits most of its polar groups on the external surfaces. As a result, the majority of the hydrophobic 'wrist' epitope are buried within the hydrophobic core, which might affect the bioactivity of rhBMP-2. If the protein molecule is bound to SWNTs-$CH_3$ or SWNTs-COOH surface, the conformation of rhBMP-2 would change by partially unfolding. Due to the shape of rhBMP-2, two possible adsorption orientations may be achieved after adsorption: side-on, with its long axis parallel to the axis of the substrates, or end-on, with its long axis perpendicular to the axis of the substrates. In the case of SWNTs-COOH, the strong interactions between the positively charged residues (Lys3, Lys5, Lys8, Lys11, Lys15 and Arg7, Arg9) and negatively charged SWNTs-COOH might give rise to a rapid binding and ensuing a mixture of "side-on" and "end-on" orientations. The lower coverage of "end-on" orientation might lead to a relative high loading amount. Meanwhile, since these positively charged residues mainly concentrate near the α3-helical region and Trp 28, Trp 31 residues, the α-helical structure and Trp-based fluorescence were greatly affected. But upon binding to the SWNTs-$CH_3$, the hydrophobic amino acid groups from the outer layer most likely interact with the hydrophobic surface and rhBMP-2 tends to show a 'side-on' orientation. In this particular orientation, a large surface area of contact is favorable for the surface interactions and thus led to a low saturation loading and unfolding of β sheets/β turns. With the unfolding of α-helical and β sheets, it is therefore possible that the hydrophobic pocket on the rhBMP-2 molecule might be opened to make the active sites of some rhBMP-2 accessible to the cellular receptors. This favors the interactions of BMP-2 and cellular receptors and thus enhancing ALP expression. Therefore, we hypothesized that the opposite electrostatic potential between the SWNTs-COOH and rhBMP-2 could contribute decisively to the alteration of the conformation and bioactivity of rhBMP-2, while the hydrophobic-hydrophobic interactions might play critical role on the change of conformation and bioactivity of rhBMP-2 on the SWNTs-$CH_3$ surface.

Once released, rhBMP-2 proteins were exposed to water again and tended to restore their native-type conformations. This resulted in the decreased bioactivity. But it is not clear yet why different conformation remaining for rhBMP-2 released from SWNTs-COOH or SWNTs-$CH_3$, and further investigations are needed to reveal their conformational evolution difference.

In conclusion, we found the adsorption dynamics, changes of conformation, orientation and the bioactivity of rhBMP-2 upon adsorption on various SWNTs surface. It provides new routes (e.g., via modulating the properties of the substrate) on the efficient immobilization and dosage reduction of rhBMP-2. Further understanding the interface between biomaterials and rhBMP-2, the subsequent cell adhesion and tissue regeneration may be regulated.

## Acknowledgments

The authors wish to express their gratitude to the financial supports from National Basic Research Program of China (973 Program, No. 2012CB933600), National Natural Science Foundation of China (Nos. 31070850, 31100679). This study was also supported by Program for New Century Excellent Talents in University (No NCET-11-0640) and the Scientific Foundation for the Returned Overseas Chinese Scholars of State Education Ministry.

## Appendix A. Supplementary data

Supplementary data associated with this article can be found, in the online version, at http://dx.doi.org/10.1016/j.bbrc.2013.09.036.

## References

[1] F. Oliveira, S. Gemming, G. Seifert, Conformational analysis of aqueous BMP-2 using atomistic molecular dynamics simulations, J. Phys. Chem. B. 115 (2010) 1122–1130.
[2] S. Facca, C. Cortez, P.C. Mendoza, N.D. Messadeq, Activity multilayered capsules for *in vivo* bone formation supporting information, PNAS 107 (2010) 3406–3411.
[3] Y.M. Kolambkar, J.D. Boerckel, K.M. Dupont, Spatiotemporal delivery of bone morphogenetic protein enhances functional repair of segmental bone defects, Bone 49 (2011) 485–492.
[4] T. Crouzier, A. Szarpak, T. Boudou, Polysaccharide-blend multilayers containing hyaluronan and heparin as a delivery system for rhBMP-2, Small 6 (2010) 651–662.
[5] D. Ben-David, S. Srouji, K. Shapira-Schweitzer, O. Kossover, E. Ivanir, G. Kuhn, R. Müller, D. Seliktar, E. Livne, Low dose BMP-2 treatment for bone repair using a PEGylated fibrinogen hydrogel matrix, Biomaterials 34 (2013) 2902–2910.

[6] J.D. Boerckel, Y.M. Kolambkar, K.M. Dupont, B.A. Uhrig, E.A. Phelps, H.Y. Stevens, A.J. García, R.E. Guldberg, An alginate-based hybrid system for growth factor delivery in the functional repair of large bone defects, Biomaterials 32 (2011) 5241–5251.
[7] Y.M. Kolambkar, J.D. Boerckel, K.M. Dupont, M. Bajin, N. Huebsch, D.J. Mooney, D.W. Hutmacher, R.E. Guldberg, Spatiotemporal delivery of bone morphogenetic protein enhances functional repair of segmental bone defects, Bone 49 (2011) 485–492.
[8] W. Shang, J.H. Nuffer, V.A. Mun˜iz-Papandrea, W. Colón, R.W. Siegel, J.S. Dordick, Cytochrome C on silica nanoparticles:influence of nanoparticle size on protein structure, stability, and activity, Small 5 (2009) 470–476.
[9] Z.J. Deng, M.T. Liang, M. Monteiro, I. Toth, R.F. Minchin, Nanoparticle-induced unfolding of fibrinogen promotes Mac-1 receptor activation and inflammation, Nat. Nanotechnol. 6 (2011) 39–44.
[10] P. Roach, D. Farrar, C.C. Perry, Surface tailoring for controlled protein adsorption: effect of topography at the nanometer scale and chemistry, J. Am. Chem. Soc. 128 (2006) 3939–3945.
[11] S.S. Karajanagi, A.A. Vertegel, R.S. Kane, J.S. Dordick, Structure and function of enzymes adsorbed onto single-walled carbon nanotubes, Langmuir 20 (2004) 11594–11599.
[12] G. Grigoryan, Y.H. Kim, R. Acharya, K. Axelrod, R.M. Jain, L. Willis, M. DrndicJ.M. Kikkawa, W.F. DeGrado, Computational design of virus-like protein assemblies on carbon nanotube surfaces, Science 332 (2011) 1071–1076.
[13] H.Q. Peng, L.B. Alemany, J.L. Margrave, V.N. Khabashesku, Sidewall carboxylic acid functionalization of single-walled carbon nanotubes, J. Am. Chem. Soc. 125 (2003) 15174–15182.
[14] C. Scheufler, W. Sebald, M. Hülsmeyer, Crystal structure of human bone morphogenetic protein-2 at 2.7 Å resolution, J. Mol. Biol. 287 (1999) 103–115.
[15] T. Kirsch, J. Nickel, W. Sebald, BMP-2 antagonists emerge from alteration in the low-affinity binding epitope for receptor BMPR-II, EMBO. J. 19 (2000) 3314–3324.
[16] J. Massagué, TGF-β signal transduction, Annu. Rev. Biochem. 67 (1998) (2000) 753–791.
[17] A.H. Reddi, Bone morphogenetic proteins: an unconventional approach to isolation of first mammalian morphogens, Cytokine Growth Factor Rev. 8 (1997) 11–20.
[18] H.J. Zhou, J.C. Qian, J. Wang, C.S. Liu, Enhanced bioactivity of bone morphogenetic protein-2 with low dose of 2-N, 6-O-sufated chitosan *in vitro* and vivo, Biomaterials 30 (2009) 1715–1724.
[19] K. Kashiwagi, T. Tsuji, K. Shiba, Directional rhBMP-2 for functionalization of titanium surfaces, Biomaterials 30 (2009) 1166–1175.
[20] W. Shang, J.H. Nuffe, J.S. Dordick, Unfolding of ribonuclease A on silica nanoparticle surfces, Nano. Lett. 7 (2007) 1991–1995.
[21] A.H. Reddi, Role of morphogenetic proteins in skeletal tissue engineering and regeneration, Nat. Biotechnol. 16 (1998) 247–252.
[22] S. Keller, J. Nickel, J.L. Zhang, Molecular recognition of BMP-2 and BMP receptor IA, Nat. Struct. Biol. 11 (2004) 481–488.